High-Stress Piezoresistance and Mobility in Degenerate Sb-Doped Germanium*

M. CUEVAS
Institute for the Study of Metals, University of Chicago, Chicago, Illinois
AND
H. FRITZSCHE
Department of Physics and Institute for the Study of Metals, University of Chicago, Chicago, Illinois
(Received 1 October 1964)

The resistivity of germanium containing between $N=3\times10^{17}$ and 10^{19} antimony atoms per cc was measured at 1.2°K under uniaxial compressions of up to 10^{10} dyn cm^{-2}. These stresses are high enough to effect an observable saturation in the piezoresistance, that is, to transfer all electrons to a single conduction-band valley ([111] compression) or to two valleys ([110] compression). Two distinct ranges are observed in degenerate germanium: for $N<10^{18}$ cm^{-3} the mobility increases with N and shows impurity-band effects; for $N>10^{18}$ cm^{-3} the mobility decreases and ionized-impurity scattering is the dominant scattering process. The latter range is $N>3\times10^{18}$ cm^{-3} for large [111] compression. The resistivity was measured for current flowing parallel and perpendicular to the stress direction. The mobility anisotropy was found to be $\mu_1/\mu_{11}=3.9\pm0.1$ for $N>4\times10^{18}$ cm^{-3}. This indicates that the mean free path is nearly isotropic. The mobility for electrons in 1, 2, and 4 valleys is compared with Csavinszky's partial-wave treatment of impurity scattering. The change of screening with the number of valleys was taken into account. Csavinszky's theory overestimates the N dependence and the magnitude of the scattering. This is attributed to the failure of the individual-scattering assumption.

I. INTRODUCTION

THE transport properties and the shape of the band edges in heavily doped (degenerate) semiconductors are not understood. Several recent experiments indicate rather significant deviations from the simple model which treats the doped semiconductor as a metal under residual resistance conditions. A negative longitudinal and transverse magnetoresistance[1] has been observed within a wide concentration range, the resistivity exhibits a temperature dependence[2] well below the degeneracy temperature, and the tunneling experiments[3] require for their explanation a sizeable number of tail states[4] extending far into the forbidden gap of the pure material. Other experiments, on the other hand, in particular the study of the piezoresistance,[5,6] the specific heat,[7] the magnetic susceptibility,[8] and the strain-induced birefringence,[9] are explained on the basis of the simple degenerate model.

The transport properties of multivalley semiconductors are complicated by the fact that the total mobility is composed of the anisotropic mobilities of each valley and that both intra- and intervalley scattering can occur, each process with a different anisotropy and different dependencies on energy and impurity concentration. It has been shown,[2,6] however, that by extending the piezoresistance measurements in degenerate germanium to stresses sufficiently high so that the electrons are transferred to two or a single conduction band valley depending on the stress orientation, the mobility anisotropy can be measured directly.

In this paper we report high-stress piezoresistance measurements in Sb-doped germanium at 1.2°K. The range of concentrations extends from 3×10^{17} to 9×10^{18} cm^{-3}. Uniaxial compressional stresses of up to 10^{10} dyn/cm^2 were used. These are sufficiently high to transfer all electrons into two valleys ([110] stress orientation) or one valley ([111] orientation). The resistivity was measured parallel and perpendicular to the stress orientation. Samples were also measured under [100] stress in order to test the homogeneity of the stress distribution and to determine the magnitude of small contributions to the piezoresistance which do not depend on the removal of the equivalence of the valleys.

Sb rather than As or P was chosen as donor element because its small central cell potential[10] yields an intervalley scattering which is negligible[11] in comparison with the intravalley scattering.

The results are compared with the ionized impurity scattering theory of Brooks and Herring[12] which is

* This work was sponsored by the U. S. Air Force Office of Scientific Research through Grant No. AFOSR 62-178.

[1] W. Sasaki and Y. Kanai, J. Phys. Soc. Japan **11**, 894 (1956); W. Sasaki, C. Yamanouchi, and G. M. Hatoyama, in *Proceedings of the International Conference on Semiconductor Physics, Prague, 1960* (Academic Press Ltd., London, 1961), p. 159; J. F. Woods and C. Y. Chen, Phys. Rev. **135**, A1462 (1964).

[2] S. H. Koenig, in *Proceedings of the International Conference on Semiconductor Physics, Exeter, 1962* (The Institute of Physics and The Physical Society, London, 1962), p. 5.

[3] R. A. Logan and A. G. Chynoweth, Phys. Rev. **131**, 89 (1963).

[4] For references see E. O. Kane, Phys. Rev. **131**, 79 (1963).

[5] O. N. Tufts and E. L. Stelzer, Phys. Rev. **133**, A1705 (1964); M. Pollack, *ibid.* **111**, 798 (1958).

[6] H. Fritzsche and M. Cuevas, in *Proceedings of the International Conference on the Physics of Semiconductors, Exeter, 1962* (The Institute of Physics and The Physical Society, London, 1962), p. 29.

[7] N. Pearlman and P. H. Keesom, Phys. Rev. **88**, 398 (1952).

[8] R. Bowers, Phys. Rev. **108**, 683 (1957).

[9] K. J. Schmidt-Tiedemann, Phys. Rev. Letters **7**, 372 (1961).

[10] P. J. Price, Phys. Rev. **104**, 1223 (1956); H. Fritzsche, *ibid.* **120**, 1120 (1960); P. Csavinszky, J. Phys. Soc. Japan **16**, 1865 (1961).

[11] W. P. Mason and T. B. Bateman, Phys. Rev. **134**, A1387 (1964); P. J. Price and R. L. Hartman, Phys. Chem. Solids **25**, 567 (1964).

[12] H. Brooks, in *Advances in Electronics and Electron Physics*, edited by L. Marton (Academic Press Inc., New York, 1955), Vol. 7, p. 85; R. B. Dingle, Phil. Mag. **46**, 831 (1955).

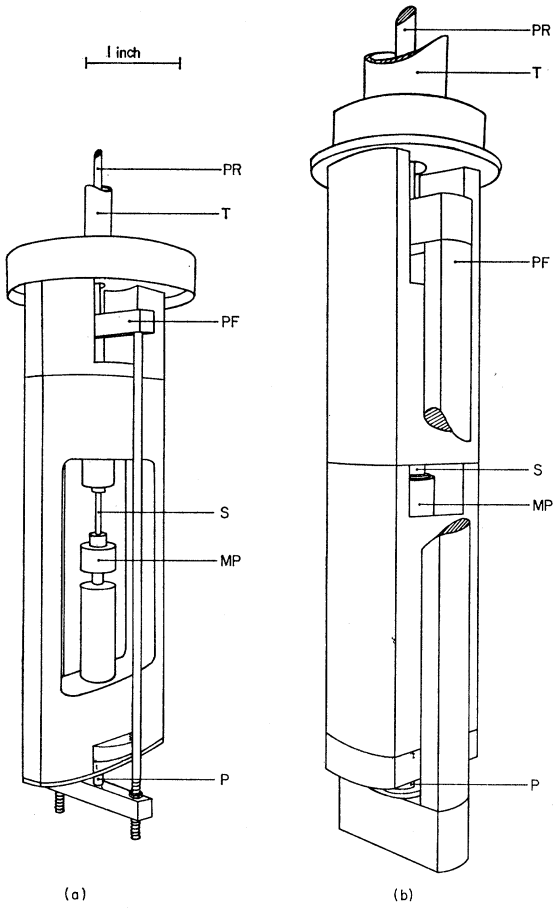

FIG. 1. Compression apparatus for (a) longitudinal and (b) transverse measurements. PR=pulling rod, T=support tubing, PF=pulling frame, S=sample, MP=movable piston, P=pin pushing the movable piston upwards.

based on the Born approximation and the more accurate partial-wave analysis of Csavinszky.[13] In both cases the change of the screening parameter with the change of the number of valleys as discussed by Robinson and Rodriguez[14] was taken into account. In both theories the scattering anisotropy was treated on the assumption of an isotropic scattering cross section.

II. STRESS APPARATUS AND CRYOSTAT

Germanium can be subjected to very large elastic strains without breakage if the surface is smooth and free of cracks. The presence of soldered leads on the surface increases the probability of breaking, but strains of the order of 10^{-2}, that is, uniaxial compressional stresses of 10^{10} dyn/cm^2, can safely be applied. The part of the stress apparatus holding the sample is shown schematically in Figs. 1(a) and 1(b) for longitudinal and transverse piezoresistance measurements, respectively. In both cases uniaxial compression is achieved by pulling the lower end of the sample upwards, holding the upper end fixed against the support of a stainless steel tubing. The pulling frame hangs on a thin stainless rod from one side of a beam balance which is on top of the cryostat but still inside the helium chamber. This construction has several advantages. First the larger tubing being under compression and the inner rod being under tension, the dimensions can be chosen so that the heat flux to the lower parts of the cryostat is very small. The inner rod would have to be much thicker to support large compressions without bending. Second, friction is eliminated by avoiding the passage of the pulling rod through a vacuum tight seal.

The compression frame of Fig. 1(a) is machined out of Invar. The ends of the sample, which has a cross section of about 0.8 mm^2 and a length of 2 cm, are cemented with Epoxy Resin into brass cups. For electrical insulation, these are placed into thin nylon cups and tightly fitted into the end holes of the movable pistons of the compression frame. Rotation of the pistons while the Epoxy is setting assures very good alignment of the sample.

The frame of Fig. 1(b) for transverse measurements is made of hardened stainless steel. The gliding surfaces of the piston and of the hole are chrome plated and polished. In this case the sample rests with its long axis perpendicular to the stress axis and is insulated by thin mica sheets from the upper surface of the compression frame and the top of the piston. These two surfaces are of hard permalloy. They were polished optically flat and parallel. For the transverse measure-

TABLE I. Sample characteristics.

Sample	N (10^{18} cm^{-3})	E_{F_0}[a] (eV)	$E_{F_{sat}}$[b] (eV)	μ_0 at 1.3°K[a] (cm^2 sec^{-1} V^{-1})	μ_{sat} at 1.3°K[b] (cm^2 sec^{-1} V^{-1})
Sb-C-a	0.320	0.00303	0.0048	809.5	326
Sb-C-b	0.845	0.0058	0.0093	1127	517
Sb-C-1	1.10	0.00693	0.0111	1097	500
Sb-C-2	2.47	0.0119	0.0190	1077	510
Sb-C-3	3.96	0.0163	0.0262	973	468
Sb-C-4	5.07	0.0194	0.0310	925	459
Sb-C-5	8.38	0.0270	0.0430	848	469
Sb-F-a	0.282	0.0028	0.00705	719	56.2
Sb-F-b	0.657	0.0049	0.0123	1057	144.5
Sb-F-1	1.13	0.00705	0.0180	1056	164
Sb-F-2	1.60	0.00895	0.0227	1093	201
Sb-F-3	2.47	0.0109	0.0305	1103	219
Sb-F-4	4.27	0.0171	0.0440	1003	233
Sb-F-5	5.24	0.0199	0.0500	938	221
Sb-F-6	7.00	0.0240	0.0605	867	215
Sb-G-1	4.01	0.0164	0.0422	1046	969
Sb-G-2	4.12	0.0169	0.0430	1047	970
Sb-G-3	4.84	0.0190	0.0480	864	827
Sb-G-4	8.74	0.0282	0.0714	850	794
Sb-H-1	8.38	0.0270	0.0430	845	719

[a] The subscript 0 stands for zero stress.
[b] The subscript "sat" stands for saturation.

[13] P. Csavinszky, Phys. Rev. **131**, 2033 (1963); **135**, AB3 (1964).
[14] J. E. Robinson and S. Rodriguez, Phys. Rev. **135**, A779 (1964).

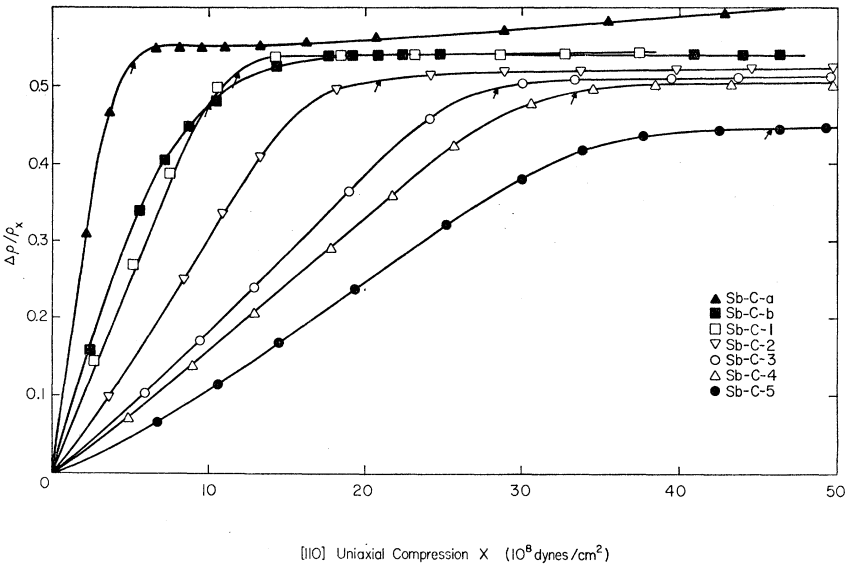

FIG. 2. Longitudinal piezoresistance as a function of [110] compressional stress (arrangement *C*) at 1.2°K for Sb-doped germanium. The arrows indicate the stress at which saturation is expected for parabolic bands.

ments the samples were about 0.8 cm long, 0.3 cm high (stress direction) and 0.1 cm thick. The two critical surfaces were polished flat and parallel, and the sample was then exposed to a fast, nonpreferential *CP*4 etch to remove surface damage.

III. EXPERIMENTAL RESULTS AND DISCUSSION

The samples are listed in Table I. The antimony concentration was obtained from Hall measurements at 300°K or 78°K, using $R=(en)^{-1}$. In some cases the Hall coefficient R differed by a few percent at these two temperatures. The R value of smallest magnitude was then used for the calculation of the concentration N. The uncertainty in N is approximately $\pm 3\%$.

The letters *C*, *F*, *G*, and *H* in the sample notation symbolize the various stress and current orientations as explained in Table II. This table also lists the energy shifts of the valleys caused by the shear part of the uniaxial compression X and the mobility components of the various valleys in the current direction. A shear deformation potential $E_2=19$ eV/strain as obtained[15] from lightly doped samples and the elastic shear constant[16] $S_{44}=1.47\times10^{-12}$ cm^2/dyn will be used in the following.

TABLE II. Sample notation and mobility components for different orientations of compressional stress X and current I.

Sample notation	Orientation X	Orientation I	Shift of valleys[a] with respect to zero stress position		Mobility component in current direction
C	[110]	[110]	2 up	$E_2S_{44}X/6$	$\mu_\perp$
			2 down	$-E_2S_{44}X/6$	$(\mu_\perp+2\mu_{11})/3$
F	[111]	[111]	3 up	$E_2S_{44}X/9$	$(8\mu_\perp+\mu_{11})/9$
			1 down	$-E_2S_{44}X/3$	μ_{11}
G	[111]	[1$\bar{1}$0]	3 up	$E_2S_{44}X/9$	$\mu_\perp$ (one) $(\mu_\perp+2\mu_{11})/3$ (two)
			1 down	$-E_2S_{44}X/3$	$\mu_\perp$
H	[110]	[001]	2 up	$E_2S_{44}X/6$	$(2\mu_\perp+\mu_{11})/3$
			2 down	$-E_2S_{44}X/6$	$(2\mu_\perp+\mu_{11})/3$

[a] $E_2=19$ eV is the shear deformation potential; $S_{44}=1.47\times10^{-12}$ cm^2/dyn is the shear elastic constant.

Figures 2, 3, and 4 show the relative change of the resistivity $(\rho_x-\rho_0)/\rho_x$ as a function of compressional stress X at 1.2°K for the two longitudinal cases *C* and F and for the transverse case *G*, respectively. In the absence of any band tailing, which is expected to be caused by the random distribution of impurities, one expects these piezoresistance curves to saturate when all electrons are transferred from the higher valleys to the low valley or valleys. This should occur at a critical stress value[6] for which the energy separation between the upper and lower valleys equals the Fermi energy of the lower valleys. For the cases *C* and *F* saturation occurs at stresses about 6×10^8 and 3×10^8 dyn/cm^2, respectively, higher than the theoretical value. Attributing this to tail states, one concludes that about 5% of the electrons are in states spread over 3 ± 1 meV below the band edge. A much smaller number of states which possibly are located further in the forbidden gap would not be detectable in this experiment.

In the transverse case *G*, the discrepancy between the experimental and theoretical saturation stress is as large as 25×10^8 dyn/cm^2. This is not a true effect but rather due to stress inhomogeneities which occur in the transverse stress arrangement. In order to obtain a homogeneous uniaxial compression the sample has to be free to expand sideways by an amount given by the Poisson ratio. In the longitudinal-stress measurements this condition is satisfied in the center region of the sample at distances from the sample mountings larger than $4w$, where w is the larger dimension perpendicular

[15] H. Fritzsche, Phys. Rev. **115**, 336 (1959).
[16] M. E. Fine, J. Appl. Phys. **24**, 338 (1953).

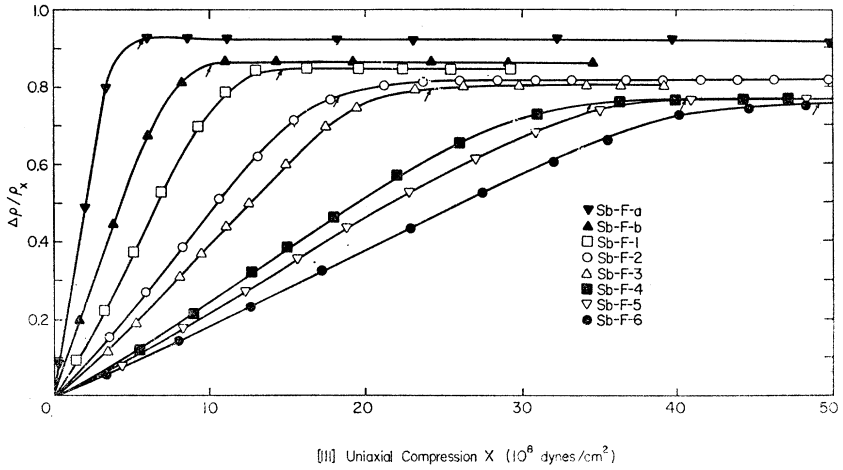

FIG. 3. Same as Fig. 2 for [111] compressional stress (arrangement F).

to the length of the sample. This condition is never satisfied in the transverse arrangement, however, since friction prevents the sample from expanding sideways at the surfaces where the compression is applied. In the Appendix, this case will be discussed in detail. It will be shown there that the piezoresistance at large stresses is not affected by the inhomogeneous stress distribution.

The piezoresistance of sample Sb-C-a shown in Fig. 2 appears to saturate near $X=8\times10^8$ dyn/cm^2. It continues to rise, however, at larger stress values. The origin of this effect, which was only observed at the low-concentration end of the range investigated, is not yet understood. This sample is not used in our later analysis.

A. Saturation Values of the Piezoresistance

Most direct information can be obtained from the piezoresistance at stresses far beyond the saturation stress where one can safely assume that all electrons are transferred to the lowest valley or valleys. Under the assumption that the total carrier concentration is unchanged by the application of stress the principal mobility components, μ_{II} and $\mu_\perp$ can be determined from the saturation $\Delta\rho/\rho_x$ of case F and G, respectively, and the component $(\mu_\perp+2\mu_{II})/3$ from that of case C (see Table II). The saturation values of $\Delta\rho/\rho_x$ remained constant at stresses above 5×10^9 dyn/cm^2. This region is not shown in Figs. 2 and 3.

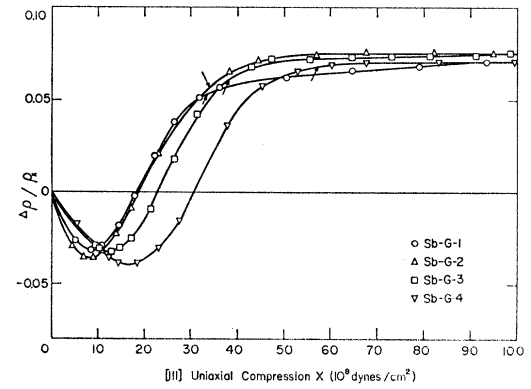

FIG. 4. Transverse piezoresistance as a function of [111] compressional stress (arrangement G) at 1.2°K for Sb-doped germanium. The arrows indicate the saturation stress for parabolic bands.

The mobility components thus determined are plotted as a function of donor or carrier concentration in Fig. 5. Also included in that figure are previously measured data points[17] of zero-stress mobility and μ_{II} of samples containing smaller N. The arrows at $N=10^{17}$ cm^{-3} and $N=2.1\times10^{17}$ cm^{-3} indicate the critical concentrations N_c for the transition[18] from nonmetallic to metallic conduction for zero stress and case F, respectively, in Sb-doped germanium. This transition is usually defined as the concentration N_c at which the thermal activation energy ϵ_2 of impurity conduction[17] vanishes. This happens when the ratio[19] $r_s/a\approx3.5$, where $r_s=(\frac{3}{4}\pi N)^{1/3}$ and $a=$effective Bohr radius. N_c is different for case $X=0$ and case F because of the reduction of a by the [111] compressional stress.[20]

It is remarkable that no break in the dependence of mobility on N accompanies the transition from nonmetallic to metallic conduction as defined in this way. The mobility, which increases rapidly with N below N_c because of the increasing overlap of the impurity wave functions continues to increase above N_c. After reaching a maximum value near $N=10^{18}$ cm^{-3} for $X=0$ and about about 3×10^{18} cm^{-3} for case F, the mobility decreases with increasing N. It is only in this higher concentration range that the mobility shows a behavior similar to an impure metal.

In the range $10^{17}\leq N\leq10^{18}$ cm^{-3}, Sb-doped Ge is metallic in the sense that the extrapolation of the resis-

[17] H. Fritzsche, Phys. Chem. Solids **6**, 69 (1958); Phys. Rev. **125**, 1552 (1962).
[18] N. F. Mott, Phil. Mag. **6**, 287 (1961).
[19] N. F. Mott and W. D. Twose, Phil. Mag. Suppl. **10**, 107 (1961).
[20] H. Fritzsche, Phys. Rev. **125**, 1560 (1962).

tivity to $T=0$ yields a finite value but the mobility of the charge carriers seems to be limited by the exchange interaction of the randomly distributed impurities. It seems unlikely that the mobility can be described by a conventional scattering theory. It is precisely in this region and at lower concentrations that the anomalous negative magnetoresistance[1] has been found in Sb-doped Ge and unusually large relaxation time anisotropies $K_\tau=\tau_{11}/\tau_\perp$ were determined from the saturation value of the longitudinal magnetoresistance.[21]

In the literature the conduction in this quasimetallic range has been called impurity band conduction[22] in contrast to hopping conduction or impurity conduction at lower concentrations. Because of their dependence on the dielectric constant and effective masses, on the number of valleys and the central cell potential of the impurity element, the upper and lower concentration limits of these ranges depend on the semiconductor material, the doping element, and the parameters affecting the Bohr radius like stress and magnetic field.

Theoretical studies of Lax and Phillips[23] have shown that the states which lie further than E_D in the band, where E_D is the ionization energy of a single impurity, remain unaffected by the impurities, whereas some of the states which lie lower are pulled down in energy and form a tail to the band which extends into the gap. One might argue that normal metallic behavior is expected only when the Fermi level penetration into the band is larger than E_D, that is $E_F \geq E_D$. This condition is satisfied at $N \geq 1.7\times10^{18}$ for the zero-stress case and at $N \geq 4\times10^{17}$ for case F. Figure 5 shows, however, that for case F the metallic behavior is only approached at concentrations $N \geq 3\times10^{18}$ which are considerably higher than for the zero stress case. Hence other factors seem to play a more important role.

In the following we restrict the analysis to the high-concentration range where the truly metallic behavior appears to be established. The range is unfortunately limited at the upper end by the relatively low solubility of Sb in Ge. The ratio of the mobilities measured in cases G and F yields directly the mobility ratio $K=\mu_\perp/\mu_{11}$. The scatter of data points in Fig. 5 is largely due to the scatter of the zero-stress resistivity as a function of concentration. The saturation values of $\Delta\rho/\rho_x$ as a function of N shown in Fig. 6 fall much better on a smooth curve. The large number of zero-stress data points make it possible to determine μ_0 quite accurately as a function of N. This curve was taken together with the smooth curves of Fig. 6 to determine the dependence of mobility on concentration for the cases C, F, and G. The mobility anisotropy K obtained from measurements G and F is $K=3.9\pm0.1$ for $4\times10^{18} \leq N \leq 9\times10^{18}$. We noticed a

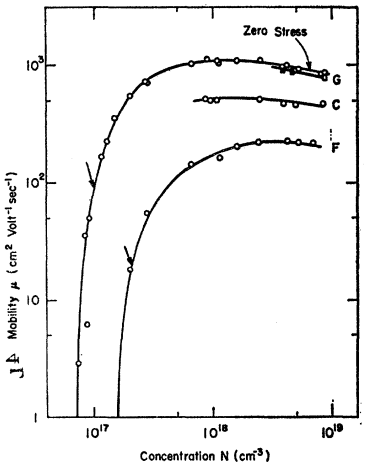

FIG. 5. Mobility components along the current direction determined from zero-stress measurements and the saturation values of the piezoresistance in arrangements C, F, and G. The arrows indicate the critical concentrations N_c at which the transition from nonmetallic to metallic conduction occurs.

slight decrease of K from $K=4.0$ to $K=3.8$ as N increases within this concentration range. This change lies, however, within the error limits.

Our value $K=3.9\pm0.1$ agrees quite well with the value $K=4.3$ quoted by Koenig[2] for Sb-doped Ge, $N=2.2\times10^{18}$ cm^{-3}. Tsidilkovsky[21] obtained $K=2$ for $N=2.4\times10^{18}$ from the saturation value of the longitudinal magnetoresistance. He finds that K decreases smoothly from $K=6$ to $K=2$ as N increases from 2.5×10^{17} to 2.4×10^{18}, whereas we find a negligible N dependence at somewhat higher N. Although his high-concentration sample lies beyond the range of impurity band conduction it is possible that at high magnetic fields the range limit is shifted to higher concentrations because of the tightening of the electron orbits. His results might therefore be affected by impurity band effects.

We determined K under conditions at which all electrons are in a single lower valley. Since we observed hardly any concentration dependence of K it seems justified to assume that K is quite insensitive to a change in screening and hence to a change in the number of valleys. If this is true one can use $K=3.9$ for the determination of μ_{11} from the mobility components

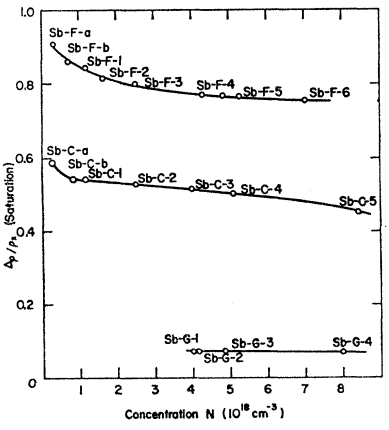

FIG. 6. Saturation values of the piezoresistance for arrangements C, F, and G as a function of carrier concentration.

[21] I. M. Tsidilkovski and V. I. Sokolov, International Conference on the Physics of Semiconductors, Paris, 1964 (unpublished).

[22] Y. Toyozawa, *Proceedings of the International Conference on Semiconductor Physics, Prague, 1960* (Academic Press Ltd., London, 1961), p. 215.

[23] M. Lax and J. C. Phillips, Phys. Rev. **110**, 41 (1958).

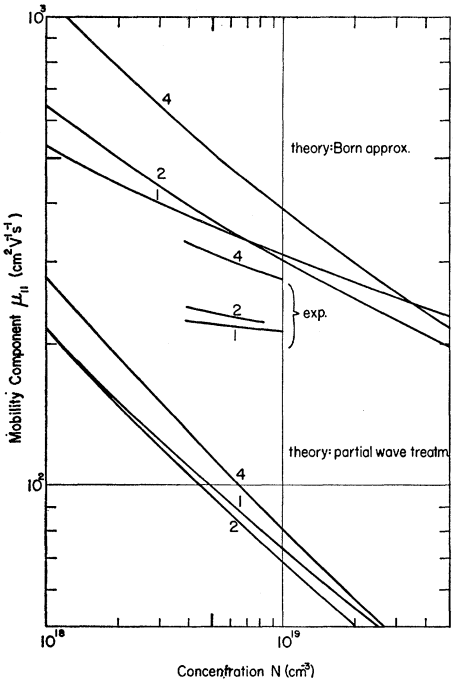

FIG. 7. Mobility component parallel to the valley axis as a function of impurity concentration. The experimental curves and the two sets of theoretical curves are marked on the figure. The numbers are the number of lower valleys.

measured at zero stress and with the C orientation. To check this assumption one sample was measured in the orientation H which is a transverse measurement with two lower valleys at saturation. From the mobility components of samples Sb-C-5 and Sb-H-1 we obtained $K=4.3\pm0.3$ for two lower valleys. This value lies slightly higher. It has, however, a larger uncertainty since the value does not represent an average over a number of measurements. Noting that this problem has not yet been clarified we shall use the assumption of a constant K in the following analysis. From the zero-stress mobility μ_0 and the mobility μ_c of arrangement C the parallel mobility components $\mu_{II}(4)$ and $\mu_{II}(2)$ for four and two lower valleys, respectively, can be determined.

$$\mu_0=\mu_{II}(4)(2K+1)/3\,,\qquad \mu_c=\mu_{II}(2)(K+2)/3\,. \tag{1}$$

The mobility values μ_{II} for one, two, and four lower valleys are shown as a function of N in Fig. 7. One notices that $\mu_{II}(4)$ lies considerably higher than $\mu_{II}(2)$ and $\mu_{II}(1)$. There are two effects that cause the mobility to depend on the number of valleys over which a given concentration of electrons is distributed. (a) The Thomas-Fermi screening radius R decreases with increasing density of states and hence with increasing number of valleys ν

$$R=(\kappa/4\pi e^2 g(E))^{1/2}\,,\qquad g(E)=\text{const}\nu^{2/3}\,, \tag{2}$$

where κ=static dielectric constant and $g(E)$=density of states. This effect indeed yields $\mu_{II}(4)>\mu_{II}(2)>\mu_{II}(1)$. Counteracting this screening effect, however, is the fact (b) that Coulomb scattering is more effective for lower energy than for higher energy carriers. Because $E_F(\nu)=E_F(1)\nu^{-2/3}$ this factor tends to make $\mu_{II}(1)$ larger than $\mu_{II}(4)$. The magnitudes and the relative importance of the two competing effects (a) and (b) can be estimated best by studying the predictions of the theories for ionized impurity scattering in degenerate semiconductors.

B. Ionized Impurity Scattering in the Born Approximation and the Partial-Wave Analysis

All scattering theories available for this problem assume that scattering occurs on N individual scattering centers, each having a total scattering cross section A. The relaxation time τ is then evaluated from

$$\tau=1/vNA, \tag{3}$$

where v is the velocity of the incoming charge carrier. In the present case this assumption is certainly unjustified in view of the fact that the de Broglie wavelength of electrons at the Fermi level and the screening radius R are of the same order of magnitude as the average impurity separation.[2] It is therefore expected that these calculations overestimate the magnitude and the N dependence of the scattering.

Another approximation is made with respect to the scattering anisotropy. Although some attempts[24] have been made to calculate anisotropic impurity scattering in nondegenerate semiconductors, very poor agreement with experiment is obtained. For degenerate multivalley semiconductors the ellipsoidal Fermi surfaces are usually approximated by spheres containing the same number of states.[13] This means the true effective masses are replaced by the density-of-states effective mass $m^*=(m_{II}m_\perp^2)^{1/3}$.

In the following we shall include the scattering anisotropy partly by assuming an isotropic mean free path $\Lambda=1/NA$ and the full anisotropy of the Fermi velocity v_F. This yields a ratio $\tau_{II}/\tau_\perp=(m_{II}/m_\perp)^{1/2}$ and a mobility anisotropy $K=\mu_\perp/\mu_{II}=(m_{II}/m_\perp)^{1/2}$. There is some conflicting evidence concerning the change of effective masses with heavy doping[25] as determined by optical reflectivity studies. Furthermore these measurements determine only the conductivity effective mass $m_\sigma^*=(m_{II}^{-1}+2m_\perp^{-1})^{-1}$. Thus even if m_σ^* is found to be independent of N the mass ratio $m_{II}/m_\perp$ might change. Using the mass ratio of pure germanium one obtains $K=4.4$ in fair agreement with our experimental value $K=3.9\pm0.1$.

[24] F. S. Ham, Phys. Rev. **100**, 1251 (1955); A. G. Samoilovich, I. Ya. Korenblit and I. V. Dakhovskii, Dokl. Akad. Nauk SSSR **139**, 355 (1961) [English transl.: Soviet Phys.—Doklady **6**, 606 (1962)].

[25] For references on this subject see Ref. 5.

Thus using an isotropic mean free path Λ we calculated μ_{II} for 1, 2, and 4 lower valleys as a function of N following Csavinszky's treatment[13] of the partial-wave analysis but including the dependence of screening on the number of valleys as expressed in Eq. (2). The results are shown together with the experimental curves in Fig. 7. The same figure also shows calculations based on the less accurate Born approximation and on the above assumptions.

The experimental mobilities are considerably higher and decrease less rapidly with increasing N than those of the partial-wave treatment. This probably has to be attributed to the failure of the individual scattering assumption. In contrast to previous experience[26] the Born approximation yields a higher mobility than the partial wave treatment. Both theories predict $\mu_{II}(4) > \mu_{II}(2)$ and $\mu_{II}(1)$ because of the more efficient screening when the electrons are in 4 valleys. The effect, however, is greatly reduced by the decrease of the scattering cross section with increasing E_F. The calculated mobilities $\mu_{II}(1)$, $\mu_{II}(2)$, and $\mu_{II}(4)$ decrease with increasing N. The slope increases with the number of lower valleys. This causes $\mu_{II}(1)$ to become larger than $\mu_{II}(2)$ at some concentration and to become even larger than $\mu_{II}(4)$ at very high concentrations.

The experimental mobility curves decrease less fast than both sets of theoretical curves. This discrepancy as well as the fact that the partial-wave treatment of Csavinszky overestimates the scattering probably result from the failure of the individual scattering model.

The magnitudes of the experimental $\mu_{II}(2)$ and $\mu_{II}(4)$ of Fig. 7 depend on the choice of the mobility anisotropy ratio K in Eq. (1). If K is not constant as we assumed but increases to $K=4.4$ with the number of lower valleys then cases for which $\mu_{II}(2)<\mu_{II}(1)$ can be obtained.

C. Low-Stress Piezoresistance

Considering only the resistivity change resulting from the shear-induced shifts of the [111] conduction-band valleys,[27] one obtains for the piezoresistance coefficient $\Pi=\Delta\rho/\rho X$ in degenerate n-type germanium for the orientations denoted by F and C, respectively,

$$\Pi(F)=-\frac{2}{9}\frac{K-1}{2K+1}\left(\tfrac{3}{2}+s\right)\frac{E_2S_{44}}{E_F}, \qquad \Pi(C)=\tfrac{3}{4}\Pi(F). \tag{4}$$

Here s is the power of the explicit energy dependence of the mobility which is assumed to have the form

$$\mu=\text{const}N^rE^s. \tag{5}$$

The factor N^r expresses the explicit concentration dependence of μ. The assumption of a constant stress-independent K implies that r and s are the same for μ_{II} and $\mu_\perp$. E_F in Eq. (4) is the zero-stress Fermi energy.

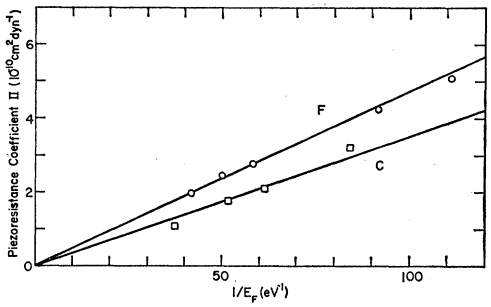

FIG. 8. The low-stress longitudinal piezoresistance coefficient as a function of reciprocal Fermi energy for [110] uniaxial compression (C) and [111] uniaxial compression (F).

The experimental values of $\Pi(F)$ and $\Pi(C)$ are plotted against $1/E_F$ in Fig. 8. From the slope of either one of these curves and the value $K=3.9\pm0.1$ the quantity s can be determined. We find $s=0.79\pm0.03$. A slightly larger value of $K=4.3$ would yield $s=0.7\pm0.03$. At low stresses the four valleys remain nearly degenerate. Since the value of s might depend on the number of lower valleys because of the change in screening, the value thus determined is $s(4)$. The slopes of the mobility curves in Fig. 7 yield the quantity $r+2s/3$ because the mobilities are determined at $E=E_F$ and $E_F\propto N^{2/3}$. With the value $s(4)=0.79$ and the slope of the $\mu(4)$ versus N curve we find $r(4)=-0.72$.

We now compare these values with those predicted by Csavinszky's theory. The theory yields an isotropic scattering cross section and hence assumes K to be stress-independent in agreement with our analysis.

The form of the mobility as expressed in Eq. (5) is fairly well justified in the concentration range $5\times10^{18}\leq N\leq10^{19}$ cm^{-3} of interest here. For the four-valley case the theory predicts $s(4)=0.3$ and $r(4)=-0.71$. A comparison with the experimentally determined values $s(4)=0.79$ and $r(4)=-0.72$ shows a rather large disagreement of the s values and a surprisingly good agreement of the r values. One would expect the failure of the individual scattering hypothesis to have a much stronger effect on r. Even in the individual scattering theory r deviates from $r=-1.0$ because of the concentration-dependent screening effects. These effects become apparent when one compares the values of r and s for different numbers of lower valleys. The theory yields $s(2)=0.52$, $r(2)=-0.82$, and $s(1)=0.59$, $r(1)=-0.85$ in the same concentration range.

Because of the close agreement of the r values we believe that the failure of the individual scattering

[26] J. M. Ziman, *Electrons and Phonons* (Clarendon Press, Oxford, England, 1962), p. 342; F. J. Blatt, Phys. Chem. Solids **1**, 262 (1957).

[27] The magnitude of effects on the piezoresistance which do not originate from a shear-induced shift of the valleys was determined by measuring the change in resistivity under [100] compression. The piezoresistance coefficient found was to be smaller than 3% of the smallest Π obtained in arrangement C. The corrections due to the stress-induced geometry change is always less than 1%. These minor corrections have been neglected in the analysis.

hypothesis is not the only cause for the disagreement between theory and experiment. In determining the s value from the Π versus E_F^{-1} curves of Fig. 8 we used the value of the mobility anisotropy K which was directly obtained from a measurement of $\mu_{II}(1)$ and $\mu_{\perp}(1)$. If K changes as the electrons are transferred from four valleys to one valley, then such a simple analysis of the experimental data is impossible.

IV. CONCLUSIONS AND SUMMARY

The mobility of Sb-doped Ge at 1.2°K increases with concentration above as well as below the critical concentration N_c at which the transition from nonmetallic to metallic conduction occurs. No change in slope marks the occurrence of this transition on the μ versus N curves. This indicates that even above N_c the mobility is governed by the exchange interaction of the randomly distributed impurities.

Only at much higher impurity concentrations, $N \geq 10^{18}$ cm^{-3} for zero stress and $N \geq 3\times10^{18}$ cm^{-3} for large [111] compressions, does the mobility decrease with increasing N and thus show the behavior expected from a metal under residual resistance conditions.

Hence there seem to exist in germanium at very low temperatures the following concentration ranges with different conduction processes:

(a) $N<10^{16}$ cm^{-3}, impurity or hopping conduction;
(b) $3\times10^{16}<N<10^{17}$ cm^{-3}, hopping conduction or impurity band conduction with the existence of a thermal activation energy ϵ_2;
(c) $10^{17}<N<10^{18}$ cm^{-3}, impurity band conduction with $\epsilon_2=0$; and
(d) $N>10^{18}$ cm^{-3}, metallic conduction similar to a metal in its residual resistance range.

The concentrations limiting these ranges are usually not sharply defined. Furthermore, they depend on the doping element and on the state of stress in the semiconductor.

The mobility anisotropy $K=\mu_{\perp}/\mu_{II}=3.9\pm0.1$ was obtained directly by measuring the resistivity component perpendicular and parallel to the valley axis at large [111] compressional stresses in the high-concentration range $4\times10^{18}\leq N\leq9\times10^{18}$ cm^{-3}. This value is close to $K=4.4$, the theoretical value obtained with an isotropic mean free path, and a mass anisotropy equal to that of pure germanium.

We obtained the explicit energy and concentration dependence of the mobility for the four-valley case assuming the mobility anisotropy K to be stress independent. Csavinsky's calculations overestimate the magnitude of ionized impurity scattering by approximately a factor of 2 and also the total dependence of the mobility on the number of scattering centers. Both of these effects indicate that the electrons do not experience scattering at independent donor ions but rather are influenced by the potentials of several ions. The analysis also indicates that the mobility anisotropy may change with the distribution of the electrons over the various valleys.

It would be interesting to compare these results on Sb-doped Ge with similar measurements[6] on As-doped Ge. It is known[28] that the mobilities of unstressed Ge doped with As are lower by a factor of 1.4 than those of Ge doped with Sb. This is attributed[29] to the large central cell potential of the As impurities which affects the intravalley scattering and which might lead to an appreciable intervalley scattering. At large [111] compressions we find, however, that the ratio $\mu_{II}(\text{Sb})/\mu_{II}(\text{As})$ is approximately 2. The fact that this ratio is larger in the one-valley case than in the four-valley case indicates that intervalley scattering does not seem to be the dominant cause for the difference in mobilities observed with different donor elements. A quantitative analysis of the measurements on As-doped Ge is complicated by the fact that the piezoresistance continues to decrease even at the highest compressional stresses and fails to saturate. This effect is not understood and requires some further study.

ACKNOWLEDGMENTS

We are grateful to P. Csavinszky for sending us his calculations prior to their publication. We thank R. N. Hall of the General Electric Laboratory and Miss L. Roth of Purdue University for the supply of some samples used in this work. It is a pleasure to acknowledge the help of the technical staff of the Low Temperature Laboratory of the University of Chicago who made the cryogenic equipment available to us and the general support of the Low Temperature Laboratory by the National Science Foundation and by the U. S. Atomic Energy Commission.

APPENDIX: STRESS INHOMOGENEITIES IN TRANSVERSE PIEZORESISTANCE MEASUREMENTS

Smith[30] performed transverse piezoresistance measurements by stressing a long sample along its axis and measuring the resistance between large area electrodes deposited on two opposite narrow sides of the sample. These electrodes were sufficiently far away from the sample ends to assure a homogeneous stress distribution between the electrodes. This method suffers from the presence of contact resistances and capacitor-type edge effects which cause the current to be not strictly perpendicular to the stress near the ends of the electrodes.

Being unable to overcome these difficulties we applied the stress along one of the smaller dimensions of an elongated rectangular bar and measured the resistivity with the usual four-probe arrangement. In this case, however, part of the current is flowing near the upper and lower surfaces of the bar over which the

[28] Y. Furukawa, J. Phys. Soc. Japan **15**, 730 (1960).
[29] P. Csavinszky, J. Phys. Soc. Japan **16**, 1865 (1961).
[30] C. S. Smith, Phys. Rev. **94**, 42 (1954).

stress is applied. These surface regions are constrained by the frictional forces which add an inhomogeneous stress field to the applied stress.

We were not able to calculate the resulting stress pattern and have to resort to a rule of thumb known to mechanical engineers in the following argument illustrated in Fig. 9. When compressional stress is applied to the *ab* surfaces which are assumed not to change their dimensions because of frictional forces, then the bar is deformed into the shape of a rectangular barrel. The curvature of the sides of an *ac* cross section is appreciable up to distances of about $3a$ from the upper and lower ends. The curvature of the sides of a *bc* cross section extends to about $3b$ from the lower and upper ends. Only when $c \gg a$, b does one find a center region of homogeneous stress.

In our case the approximate dimensions were $b=3c=9a$ with current along b. Choosing the c or stress direction along [100] we found (i) an appreciable increase in resistivity when the b or current direction was along [011] and (ii) a negligible resistivity change when it was along [010]. This anisotropy indicates that the [100] stress axis is no longer a fourfold symmetry axis under these conditions.

In order to explain this let us consider the extreme case $b \gg c \gg a$. Since $c/a \gg 1$ the largest part of the *ac* cross sections will be unaffected by the presence of the friction forces. With $c/b \ll 1$, however, the strain component u_{yy} is nearly zero. This situation can be approximated by a superposition of a homogeneous stress field along c and another along b. Neither of these stress fields can remove the equivalence of the [111] valleys and hence they cannot contribute to a sizeable

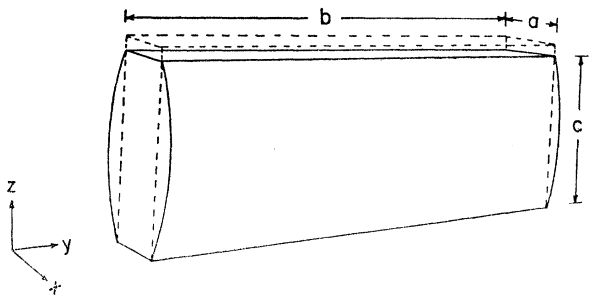

FIG. 9. Deformation of a rectangular bar under compression applied over the *ab* surfaces in the presence of large frictional forces. The small outward bulging of the *ac* surfaces is not shown in the figure.

piezoresistance in case (ii) because the stresses are along [100] and [010], respectively. In case (i) a stress along [011] appears which causes the observed increase in resistivity.

From this we conclude that the friction forces introduce additional stresses in the material. They are on the average larger along the long dimension b than along the short dimension a. We verified this by studying samples with different b/a ratios.

Under [111] compressional stress X we estimate that in our geometry an average perpendicular stress of about $0.15X$ will appear in the current direction. This means that a roughly 15% higher stress than otherwise will be required in order to reach saturation. Although the low-stress piezoresistance measurements are falsified by the stresses originating from friction, once saturation is reached the piezoresistance measurements give the correct answer.